AIAA JOURNAL
Vol. 40, No. 5, May 2002

Anisotropy-Induced Spiral Buckling in Compression-Loaded Cylindrical Shells

P. M. Weaver*
University of Bristol, Bristol, England BS8 1TR, United Kingdom

The study of axial compression buckling of isotropic cylinders has received much attention by various researchers over the years. It is commonly acknowledged that the presence of minute imperfections reduces potential buckling loads significantly in comparison with classical linear predictions. This approach has been extended by a significant, yet fewer, number of researchers to composite cylindrical shells. It is shown that imperfections may not be the only major factor for the discrepancy between experimentally obtained buckling loads and those predicted from linear bifurcation theory with orthotropic properties. Flexural/twist anisotropy, present in most balanced, symmetric laminates with angle ply layers is shown to play a significant role in reducing buckling loads from those classically predicted. Indeed, the assumption of deflections in the form of a double sine series appears to be questionable for such laminates. A previously unreported classical linear analysis including the effect of flexural/twist coupling is developed. Backed up by detailed comparison with finite element studies, it is shown that buckling loads can be reduced by up to 30% for a class of quasi-isotropic laminates and is accompanied by a change in mode form from doubly periodic to spiral in nature.

Nomenclature

A	=	$A_{11}A_{22} - A_{12}^2$
A_6	=	$A/A_{66} - 2A_{12}$
$[A_{ij}]$	=	in-plane stiffnesses
$[D_{ij}]$	=	flexural stiffnesses
h_i	=	position of ply surface in relation to midplane
l	=	length
M_{ij}	=	moment resultant
m	=	number of axial half-waves
m'	=	slope of spiral (defined in Fig. 3)
N_i	=	in-plane force resultant
n	=	number of circumferential waves
p	=	surface pressure
Q_i	=	through-thickness shear force resultant
r	=	radius
t	=	thickness
u	=	axial displacement
u_i	=	normalized ply position, h_i/t
u_0, v_0, w_0	=	maximum amplitude of wavelength
v	=	circumferential displacement
$W_1, \ldots, W_5$	=	material stiffness invariants
w	=	radial displacement
x	=	axial coordinate
y	=	circumferential coordinate
γ_{xy}	=	in-plane shear force resultant
δ, γ	=	flexural/twist anisotropy parameters [Eq. (14)]
ε_{ij}	=	in-plane direct strain resultants
θ	=	ply angle
κ_{ij}	=	out-of-plane curvatures
λ_m	=	axial wavelength [Eq. (13)]
λ_n	=	circumferential wavelength [Eq. (13)]
ξ_i	=	lamination parameter

Introduction

IT is well known that a large discrepancy exists between theoretical and experimental compressive buckling loads for isotropic cylindrical shells. Koiter[1] established that the primary reason was the effect of minute imperfections in the shell's surface. Composite shells are known to be less imperfection sensitive, presumably due to the presence of fewer potential buckling modes. Here, another deleterious effect is described that appears to be overlooked in the literature. Laminated composite cylindrical shells generally exhibit flexural/twisting coupling to some degree whenever fiber angles exist that do not lie parallel to the cylindrical axis or in a circumferential plane. Often, the effect is deemed to be small and, thus, ignored by designers, especially so when plus and minus angles are stacked adjacently. However, linear finite element (FE) analysis shows that, with even the smallest amount of coupling, the initial buckling mode changes to an asymmetric spiral pattern.[2] For a cylinder of geometry shown in Fig. 1, the double sine series (Fig. 2)

$$w = w_0 \sin(m\pi x) \sin(ny/r) \tag{1a}$$

is used to predict radial displacements in classical compression buckling analysis but is incapable of modeling asymmetric spiral modes. This is because with this equation at least one generator must remain straight with zero amplitude. However, with cylinders that exhibit asymmetric buckling deformation modes, it is necessary to generalize the expression for radial deformation. With this in mind,

$$w = w_0 \sin(ny/r - nm'x/r) \tag{1b}$$

is proposed to model normal displacements to the cylindrical surface using the cylindrical coordinate system defined in Fig. 1. There are n circumferential wavelengths, and m' is the slope of the spiral (as indicated by the line of constant amplitude). Such contours on a cylindrical surface are shown in Fig. 3. Note that such a deformation mode can not represent boundary conditions at the end of the cylinder. Although it is acknowledged that boundary conditions may significantly affect buckling loads,[3,4] the model is intended for common boundary conditions such as SS3 and fully fixed, that is, conditions that allow classical buckling loads and modes to develop. Later, it is shown that there is excellent agreement with FE results that do satisfy the boundary conditions.

The given displacement series is commonly used to model torsional buckling of cylindrical shells, but is equally valid for the spiraling mode that arises due to flexural/twist coupling under compression loads.

Derivation of Model

Equilibrium Equations

When the standard Donnell shallow-shell governing equations are used (as presented, for example, by Vasiliev[5]), shells for which

Received 14 April 2001; revision received 9 November 2001; accepted for publication 3 December 2001.

*Lecturer, Department of Aerospace Engineering, Queens Building, University Walk. Member AIAA.

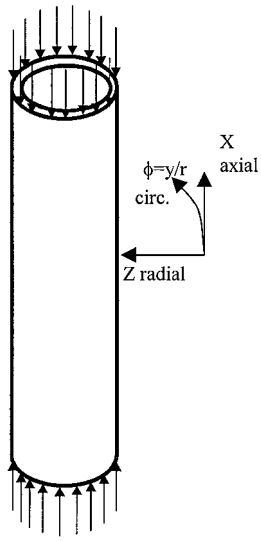

Fig. 1 Cylindrical shell subject to axial compression.

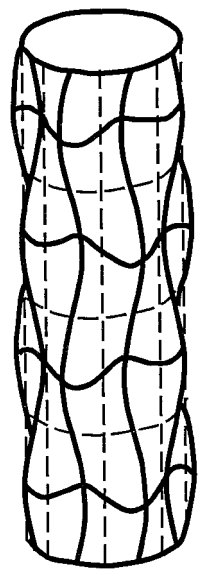

Fig. 2 Local buckling pattern characteristic of double sine series.

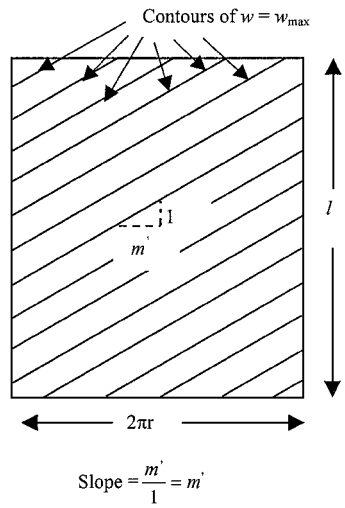

Fig. 3 Contours of maximum amplitude for spiral buckling pattern ($n = 5$); cylindrical surface projected on to two-dimensional plane. Note that left and right sides zip together.

$n > 5$ that are typical for thin-walled shells of intermediate length are considered. To understand the realms of validity of the current analysis, note that for longer shells Weaver and Dickenson[6] show that the shallow-shell assumption of negligible in-plane displacements becomes increasingly invalid for shells such that $l^2t/r^3 > 3$. For such lengths and longer, the phenomenon is easily understood in terms of an interaction between local (surface) buckling and Euler (global) buckling.

The equilibrium equations, with all terms having their usual meaning, are written as

$$\frac{\partial N_y}{\partial y} + \frac{\partial N_{xy}}{\partial x} = 0, \qquad \frac{\partial N_{xy}}{\partial y} + \frac{\partial N_x}{\partial x} = 0$$

$$\frac{\partial Q_x}{\partial x} + \frac{\partial Q_y}{\partial y} - \frac{N_y}{r} + p = 0 \tag{2a}$$

$$\frac{\partial M_{xy}}{\partial x} + \frac{\partial M_y}{\partial y} = Q_y, \qquad \frac{\partial M_{xy}}{\partial y} + \frac{\partial M_x}{\partial x} = Q_x \tag{2b}$$

Differentiating the latter two equations and adding to the first gives

$$\frac{\partial^2 M_x}{\partial y^2} + 2\frac{\partial^2 M_{xy}}{\partial x \partial y} + \frac{\partial^2 M_y}{\partial y^2} - \frac{N_y}{R} + p = 0 \tag{3}$$

as a governing equation. The expressions in Eq. (2) in conjunction with Eq. (3) represent the governing equilibrium equations of the cylindrical shell under shallow-shell assumptions and as such are identical in form to a cylindrical shell formed from any material (with anisotropy or otherwise). To introduce anisotropy into the problem, the constitutive behavior of the material is considered.

Constitutive Equations

The laminate is assumed to be balanced and symmetric such that

$$\begin{Bmatrix} N_x \\ N_y \\ N_{xy} \end{Bmatrix} = \begin{bmatrix} A_{11} & A_{12} & 0 \\ A_{12} & A_{22} & 0 \\ 0 & 0 & A_{66} \end{bmatrix} \begin{Bmatrix} \varepsilon^o_{xx} \\ \varepsilon^o_{yy} \\ \gamma^o_{xy} \end{Bmatrix} \tag{4a}$$

$$\begin{Bmatrix} M_x \\ M_y \\ M_{xy} \end{Bmatrix} = \begin{bmatrix} D_{11} & D_{12} & D_{16} \\ D_{12} & D_{22} & D_{26} \\ D_{16} & D_{26} & D_{66} \end{bmatrix} \begin{Bmatrix} \kappa_{xx} \\ \kappa_{yy} \\ \kappa_{xy} \end{Bmatrix} \tag{4b}$$

hold. A_{ij} and D_{ij} are given in terms of the material invariants W_1–W_5 and lamination parameters ξ_1–ξ_{12} (for example, Onoda[7] and Fukunaga[8]) as

$$\begin{Bmatrix} A_{11} \\ A_{12} \\ A_{22} \\ A_{66} \\ A_{16} \\ A_{26} \end{Bmatrix} = t \begin{bmatrix} 1 & \xi_1 & \xi_2 & 0 & 0 \\ 0 & 0 & -\xi_2 & 1 & 0 \\ 1 & -\xi_1 & \xi_2 & 0 & 0 \\ 0 & 0 & -\xi_2 & 0 & 1 \\ 0 & \xi_3/2 & \xi_4 & 0 & 0 \\ 0 & \xi_3/2 & -\xi_4 & 0 & 0 \end{bmatrix} \begin{Bmatrix} W_1 \\ W_2 \\ W_3 \\ W_4 \\ W_5 \end{Bmatrix}$$

$$\begin{Bmatrix} D_{11} \\ D_{12} \\ D_{22} \\ D_{66} \\ D_{16} \\ D_{26} \end{Bmatrix} = \frac{t^3}{12} \begin{bmatrix} 1 & \xi_9 & \xi_{10} & 0 & 0 \\ 0 & 0 & -\xi_{10} & 1 & 0 \\ 1 & -\xi_9 & \xi_{10} & 0 & 0 \\ 0 & 0 & -\xi_{10} & 0 & 1 \\ 0 & \xi_{11}/2 & \xi_{12} & 0 & 0 \\ 0 & \xi_{11}/2 & -\xi_{12} & 0 & 0 \end{bmatrix} \begin{Bmatrix} W_1 \\ W_2 \\ W_3 \\ W_4 \\ W_5 \end{Bmatrix} \tag{5}$$

The lamination parameters may be calculated from the following integrals:

$$(\xi_1 \quad \xi_2 \quad \xi_3 \quad \xi_4) = \frac{1}{2}\int_{-1}^{1} (\cos 2\theta \quad \cos 4\theta \quad \sin 2\theta \quad \sin 4\theta)\, \mathrm{d}u_i$$

$$(\xi_9 \quad \xi_{10} \quad \xi_{11} \quad \xi_{12}) = \frac{3}{2}\int_{-1}^{1} (\cos 2\theta \quad \cos 4\theta \quad \sin 2\theta \quad \sin 4\theta) u_i^2\, \mathrm{d}u_i$$

$$u_i = \frac{2h_i}{t} \tag{6}$$

where h_i is the distance of a particular ply surface from the midplane and t is the thickness of the laminate. Note that the flexural/twist coupling is given in terms of D_{16} and D_{26}.

The geometric equations are

$$\varepsilon_{xx} = \frac{\partial u}{\partial x}, \qquad \varepsilon_{yy} = \frac{\partial v}{\partial y} + \frac{w}{r}, \qquad \gamma_{xy} = \frac{\partial u}{\partial y} + \frac{\partial v}{\partial x}$$

$$\kappa_{xx} = -\frac{\partial^2 w}{\partial x^2}, \qquad \kappa_{yy} = -\frac{\partial^2 w}{\partial y^2}, \qquad \kappa_{xy} = -2\frac{\partial^2 w}{\partial x \partial y} \tag{7}$$

with the usual shallow-shell assumptions[4] by ignoring the contributions of v to curvatures κ_{xx} and κ_{xy}. In addition to normal displacements, we propose using

$$u = u_0 \cos(ny/r - nm'x/r)$$

$$v = v_0 \cos(ny/r - nm'x/r) \tag{8}$$

to represent the in-plane displacements.

The immediate goal is to reduce the governing equations into our unknown displacements u, v, and w, by substituting Eq. (4) into Eqs. (3) and (2) and by then substituting for the strains from Eq. (7). The three governing equations become

$$A_{11}\frac{\partial^2 u}{\partial x^2} + A_{66}\frac{\partial^2 u}{\partial y^2} + (A_{12} + A_{66})\frac{\partial^2 v}{\partial x \partial y} + \frac{A_{12}}{R}\frac{\partial w}{\partial x} = 0$$

$$A_{66}\frac{\partial^2 v}{\partial x^2} + A_{22}\frac{\partial^2 v}{\partial y^2} + (A_{12} + A_{66})\frac{\partial^2 u}{\partial x \partial y} + \frac{A_{22}}{R}\frac{\partial w}{\partial y} = 0$$

$$D_{11}\frac{\partial^4 w}{\partial x^4} + 2(D_{12} + 2D_{66})\frac{\partial^4 w}{\partial^2 x \partial y^2} + D_{22}\frac{\partial^4 w}{\partial y^4} + 4D_{16}\frac{\partial^4 w}{\partial^3 x \partial y}$$

$$+ 4D_{26}\frac{\partial^4 w}{\partial x \partial y^3} + \frac{A_{22}}{R^2}w + \frac{A_{12}}{R}\frac{\partial u}{\partial x} + \frac{A_{22}}{R}\frac{\partial v}{\partial y} - p = 0 \tag{9}$$

The first two equations represent equilibrium of the plane of the surface and as such are unaffected by flexural/twist coupling. When expressions for the in-plane displacements, u and v, from Eq. (8) are further substituted into the first two expressions in Eq. (9), it is possible to gain expressions for u_0 and v_0 in terms of w_0 as

$$\frac{u_0}{w_0} = -\frac{\lambda_m}{R}\frac{A_{12}\lambda_m^2 - A_{22}\lambda_n^2}{A_{11}\lambda_m^4 + A_6\lambda_m^2\lambda_n^2 + A_{22}\lambda_n^4}$$

$$\frac{v_0}{w_0} = +\frac{\lambda_n}{R}\frac{\left(A_{11}A_{22} - A_{12}^2 - A_{12}A_{66}\right)\lambda_m^2 + A_{22}A_{66}\lambda_n^2}{A_{66}\left(A_{11}\lambda_m^4 + A_6\lambda_m^2\lambda_n^2 + A_{22}\lambda_n^4\right)} \tag{10}$$

Note that in the state immediately after buckling there is a component of in-plane load acting radially that equilibriates the surface pressure p as

$$p = -N_x\frac{\partial^2 w}{\partial x^2} \tag{11}$$

Then, substituting for p from Eq. (11) and for u_0 and v_0 from Eq. (10) into the last expression in Eq. (9) and rearranging gives an expression for the in-plane load as

$$N_x = \left[D_{11}\lambda_m^2 + 2(D_{12} + 2D_{66})\lambda_n^2 + D_{22}\frac{\lambda_n^4}{\lambda_m^2} - 4D_{16}\lambda_m\lambda_n\right.$$

$$\left. - 4D_{26}\frac{\lambda_n^3}{\lambda_m}\right] + \left\{\frac{A\lambda_m^2}{R^2\left[A_{11}\lambda_m^4 + A_6\lambda_m^2\lambda_n^2 + A_{22}\lambda_n^4\right]}\right\} \tag{12}$$

which is the sum of two terms reflecting bending and membrane responses, respectively. Within the realms of shallow-shell theory, the presence of flexural/twist coupling is expected to affect the bending response only, as is borne out by the exclusion of D_{i6} terms in the membrane stiffnesses. The last expression is interesting because it clearly shows the destabilizing effect of flexural/twist coupling as represented by the terms involving D_{i6}. This equation is identical in all respects with the common expression for classical buckling as described, for example, by Vasiliev,[5] except for the inclusion of D_{i6} terms and the definitions of λ_m and λ_n that are given by

$$\lambda_m = m'n/r, \qquad \lambda_n = n/r \tag{13}$$

where n and r are the number of circumferential wavelengths and the radius, respectively. The m' term is the gradient of the spiral as measured by a line of constant radial amplitude. It may be defined as the ratio of circumferential to longitudinal travel for the spiral. Note that λ_m is now a continuous variable that may attain negative as well as positive values. The buckling load is found by exhaustively searching for the values of n and m' that minimize the expression for in-plane load Eq. (12). These results are compared with those obtained from FE analysis for quasi-isotropic laminates and are presented in the following section.

Results

Layup Effects

It has been shown by Weaver et al.[2] that the minimum number of unidirectional layers to obtain the optimal layup, proven by Onoda,[7] is 48. This number reflects the minimal number of plies to produce a homogeneous, specially orthotropic, quasi-isotropic layup, using only 0-, 90-, and ±45-deg plies. The layup, reproduced here in Appendix A, is nonintuitive, and the interested reader is referred to Ref. 2 for further discussion. The reason we introduce it here is that now we have a means of quantifying the effect of nonorthotropic laminates, that is, laminates that possess flexural/twist coupling, on buckling loads. The 48-ply laminate listed as laminate P in Appendix B is similar to the optimal layup in all respects except that it exhibits maximum flexural/twist coupling for the homogeneous, quasi-isotropic layup. Its predicted buckling load, as given by classical orthotropic shell theory (for example, Vasiliev[5]) is identical to that of the optimal. However, the solution of Eq. (12) shows that the true classical load is 30% lower than that of the optimal laminate. This 30% knockdown is highly significant and rather surprising at first sight. A similar, albeit numerical study by Nemeth,[9] shows that flexural/twist coupling for compression buckling of flat plates is only significant for anisotropy factors greater than 0.18. Nemeth defines the anisotropy factor as

$$\delta = D_{16}\Big/\sqrt[4]{D_{11}^3 D_{22}} \qquad \text{or} \qquad \gamma = D_{26}\Big/\sqrt[4]{D_{22}^3 D_{11}} \tag{14}$$

whichever is the larger. The same parameters are adopted in our study of cylindrical shells.

It is instructive to seek the largest value of anisotropy factor and in so doing to evaluate the largest knockdown factor. To do so, it is useful to reconsider the flexural stiffnesses in terms of their lamination parameters and material invariants [Eqs. (4) and (5)]. Note that $D_{11} = D_{22} = W_1 h^3/12$ for a homogeneous, quasi-isotropic, symmetric layup. For such a laminate, the lamination parameters ξ_1, ξ_2, ξ_9, and ξ_{10} are zero. As a consequence of homogeneity, the integration of u^2 is the same for 0- and 90-deg fiber angles. Then, the anisotropy factor can be rewritten as

$$\delta = \gamma = \left[W_2 \Big/ 2\sum_{i=1}^{n}\left(u_i^3 - u_{i-1}^3\right)\sin 2\theta_i\right] \Big/ W_1$$

where n indicates the number of fiber angles ($n = 4$, in this instance). To maximize δ (or γ), it is necessary to maximize the term within the summation term, noting that nonzero terms exist for ±45-deg plies only. Then note that this term is maximized by maximizing the difference in the second moment of areas between the +45- and −45-deg plies, which happens when either ply angle is grouped closest to the midplane. Under these circumstances it is straightforward to show

$$\delta_{\max} = \gamma_{\max} = 15W_2/64W_1 \tag{15}$$

giving a value of 0.253 for the carbon/epoxy material described in Appendix C. Because W_1 is a measure of D_{11} or D_{22} for this laminate family, it seems reasonable, particularly after noting the form of the expression for the anisotropy factor, that W_2 is a measure of flexural/twist anisotropy. This, then, is the largest value of anisotropy factor that may occur for a homogeneous, quasi-isotropic laminate, and we shall make use of this when assessing the impact of flexural/twist anisotropy on the classical local buckling capacity of cylindrical shells made from homogeneous, quasi-isotropic laminates. An example of such a laminate is given is Appendix A. For

homogeneous laminates, γ and δ will be equal, as D_{11} and D_{22} are equal. The 48-layer, symmetric, homogeneous laminates with differing magnitudes of anisotropy were used to investigate the effect D_{16} and D_{26} coupling has on the buckling load. The effect of the coupling terms, as given by the anisotropy factors (γ and δ) on buckling loads is quantified next in the investigation for quasi-isotropic laminates.

FE Analysis

The expression for the buckling load given in Eq. (12) is validated by detailed comparison with FE analyses. Conventional FE analysis practice as espoused, for example, in the ABAQUS User's Manual,[10] suggests reducing computational time by making use of symmetry within the structure. Typically, this is done in two ways. The first is to use half-length models and superimpose symmetry and antisymmetry boundary conditions at the midpoint in two separate runs. Second, a number of runs are carried out with different circumferential wave numbers. For instance, if n is anticipated to equal 5, a quarter-wave model is produced with a subtended angle of 18 deg. A number of models are run with different n values in combination with the two sets of boundary condition at the midpoint. Then, the argument goes, the true eigenmode is readily obtained as the one that minimizes the buckling load. This approach is fine in many cases, but it must be realized that it is not valid for composite laminates in general because of the presence of coupling terms that may favor an asymmetric buckling pattern. Under these circumstances, the full shell should be modeled. Related work by Jaunky and Knight[11] examined the buckling behavior of curved composite panels with r/t ratios of 50 such that they could be considered to be of intermediate length so that comparison with present results is applicable. They, too, note knockdowns due to anisotropy, but not as severe as reported here. A plausible explanation for this discrepancy is the presence of the longitudinal edge conditions in the curved panels that eliminate displacements and force the buckling mode to be bidirectional. Note that the double sine series can be used to model such buckling modes, but the present work suggests that the whole panel should be modeled because anisotropy eliminates midlength symmetry. A further criticism of using symmetry conditions to reduce computational effort is that they may not accurately model buckling of cylindrical shells that is precipitated by a mode that is localized longitudinally. So-called homoclinic buckling mechanisms have been extensively studied in isotropic shells in recent years.[12,13]

The FE analysis used was ABAQUS Standard.[10] The dimensions of the cylinders modeled were length of 400 mm, radius of 40 mm, and thickness of 1 mm. These dimensions were chosen to avoid any interaction between local buckling and other failure modes such as Euler and shear buckling. The materials properties are listed in Appendix C.

The model was constructed of parabolic thick shell elements (S8R)[10] that allowed a linear variation of stress across the element and through thickness stresses and shear deformation to be modeled. The analyses were repeated with S8R5[10] elements that do not model transverse shear deformation. There was negligible difference in buckling loads, suggesting that shear deformation effects were negligible. Circumferentially, these models had 36 elements and axially had 100 elements. This ensured that the aspect ratio of the elements was kept close to unity. The use of rigid elements (R3D3)[10] at the ends of the tubes formed the equivalent of platens relative to which the support and loading conditions could be defined. For the tests carried out, fully fixed supports allowing axial displacement at one end were defined. A mesh refinement study was conducted to ensure satisfactory convergence had been achieved as measured by comparison of results/buckling pattern with the analytical solution (12). FE results obtained lie within 2% of the analytical predictions and, thus, validate the analytical model. Typical spiral buckling modes obtained by FE are given in Fig. 4, noting that displacements are greatly exaggerated. The results indicate that the angle of the spiral increases with anisotropy factor. The general form of such patterns is predicted by Eq. (1b). The only difference is the presence of an additional overall sinusoidal variation of one-half wavelength axially, predicted by FE, that removes displacements at the cylinder's ends. Although not modeled analytically, the number of circumferential

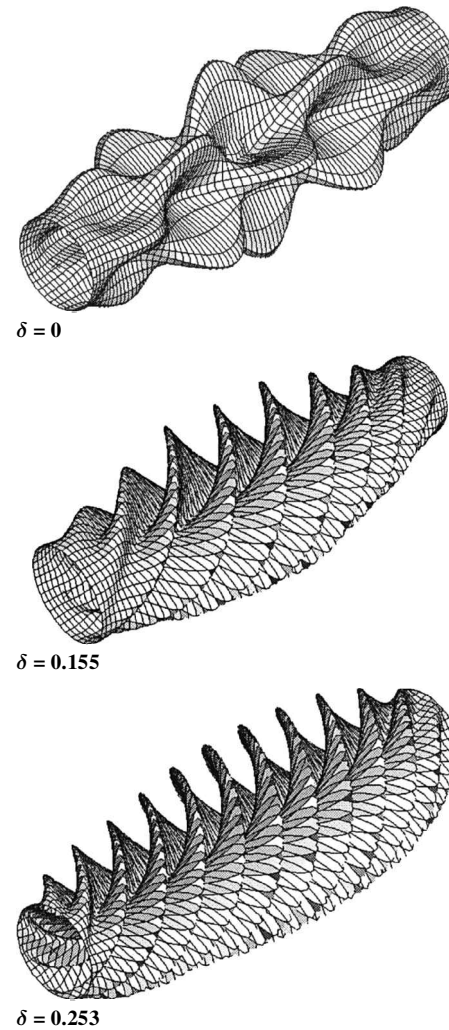

Fig. 4 Spiral buckling due to the effects of flexural/twist anisotropy; degree of spiraling increases for increasing anisotropy.

wavelengths and the slope of the spiral are identical with that predicted by FE with appropriate SS3 boundary conditions. This result suggests that the usual simply supported conditions exert little influence on the character of these buckling mode shapes. A parallel study on usual clamped conditions (C3 condition)[3] showed similar results.

Classical Analysis

Having established that the buckling load predicted by Eq. (12) matches those obtained by FE analysis, the effect of flexural/twist coupling on homogeneous, quasi-isotropic laminates is examined. This class of laminates is important, because according to classical linear buckling analysis (for example, Vasiliev[5]), this class of laminates gives the highest buckling load.[7] However, this classical buckling analysis neglects the effect of flexural/twist coupling. Therefore, by the use of Eq. (12), the effects of flexural/twist coupling may be assessed.

To examine the effect of flexural/twist coupling on quasi-isotropic laminates, a sample of 30 different 48-layer laminates, each homogeneous, that is, $D_{ij}/A_{ij} = t^2/12$ with $ij \neq i6$, were studied. These are listed in Appendix B. According to classical linear buckling analysis, using Vasiliev's formula,[5] all of these laminates are optimal and give the same maximum buckling load. However, when Eq. (15) is used, it is obvious that this is not the case. A plot of knockdown factor due to flexural/twist anisotropy k_D against anisotropy factor is shown in Fig. 5. A monotonic relationship is clearly observed. The maximum value of anisotropy factor ($D_{16}/\sqrt[4]{(D_{11}^3 D_{22})} = 0.253$) for quasi-isotropic laminate has the largest knockdown factor of 30%. A design formula is readily derived by simple linear regression:

$$N_{\text{flex/twist}} = N_{\text{maximum}}\left[1 - 1.165\left(D_{16}\Big/\sqrt[4]{D_{11}^3 D_{22}}\right)\right] \qquad (16)$$

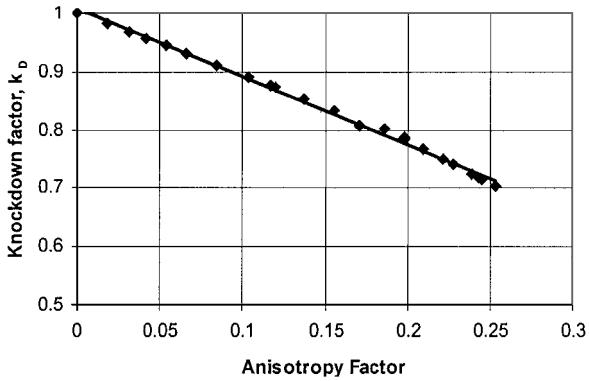

Fig. 5 Knockdown effect of flexural/twist buckling on classical analysis for homogeneous quasi-isotropic laminates.

where N_{maximum} is obtained for the homogeneous, quasi-isotropic laminate with zero anisotropy.

The correlation coefficient is high at 0.997 for SS3 boundary conditions. Note, however, that this expression is only valid for the restricted class of homogeneous, quasi-isotropic laminates within the realms of Donnell's shallow-shell theory.[11] Specifically, l^2t/r^3 must be small, typically less than 3, and the Batdorf[14] parameter must not be small, that is, $l^2/rt > 100$. Note that these are approximate numbers that are affected by orthotropy and anisotropy. A further restriction is placed on the applicability of the analytical model by the neglect of boundary conditions, particularly on the radial displacement w. Specifically, the ratio of the spiral wavelength to length of the tube, as found from Eq. (12), should be small, as expressed by $nm'l/r \ll 1$. For the remainder of this discussion, cylinders that obey these criteria are referred to as cylinders of intermediate length. Each laminate that is represented by a data point in Fig. 5 is identified in Appendix D. From Eq. (16), it appears that a value of γ, $\delta = 0.18$ gives a knockdown in buckling load of approximately 20%. Figure 5 is highly significant because it shows that flexural/coupling is more significant in cylindrical shells than flat plates, where the knockdown is nearer 2% (Ref. 9).

It appears that this spiral mode has not been observed experimentally in quasi-isotropic shells. Provisional experimental work on $(\pm 45)_s$ carbon/epoxy laminated shells[15] clearly shows the presence of a localized spiral buckling mode. When repeated for a $(\pm 45, 0, 90)_s$ quasi-isotropic laminate, the observation of buckling mode shape was inconclusive because material failure occurred very quickly after buckling. Nonlinear postbuckling FE studies, however, appear to show a mode jump from one that is spiral in nature to one that is doubly periodic.[16] Perhaps herein lies the explanation of why it has not been observed previously. Additional investigations are under way to further examine this phenomenon. Recently, Hilberger and Starnes[17] reported experimental and dynamic buckling studies using FE, on a carbon/epoxy laminated cylinder. The layup was quasi isotropic $(\pm 45, 0, 90)_s$ and of proportions such that local buckling occurred. Unfortunately, the proportions of the cylinder render the current analysis invalid because $nm'l/r$ as predicted by Eq. (12) is no longer small valued, as is required by the analysis presented herein. The physical interpretation of this is that boundary conditions on radial displacement can not be ignored as they are in Eq. (1b). It does appear that anisotropy effects were less important in their tests as compared with the prediction of Eq. (12). They report a knockdown of 5% due to anisotropy, as compared with a value of 19% predicted by Eq. (12). This difference is believed to be due to nonsatisfaction of the boundary conditions of the analysis presented here.

It does appear then that anisotropy effects are influential on buckling loads and may be as significant as the presence of imperfections, especially for cylinders of intermediate length.

Conclusions

In conclusion, a classical linear analytical formula has been derived for axial compression buckling of laminated cylindrical shells that includes the deleterious effect of flexural/twist coupling. Its applicability is restricted to shells of proportions such that shallow shell theory holds. Furthermore, $nm'l/r \ll 1$ so that the assumption of neglecting end conditions is valid. This model has been verified in comparison with linear FE analyses. A detailed study of flexural/twisting effects in optimal quasi-isotropic laminates was undertaken and found to have potentially adverse effects of up to 30%. For similar values of anisotropy factors, it should be recognized that flexural/twisting anisotropy potentially has greater harmful effects in a shell than plated structures.

Appendix A: Optimal Layup

The 48-layer, symmetric, homogeneous, specially orthotropic laminate is

$(0, -45, 90, +45, 0, -45, +45, 90, -45, 90, +45, +45,$
$90, 0, 0, 90, +45, -45, +45, -45, 0, 0, 90, -45)_s$

Appendix B: Homogeneous Layups with Flexural/Twist Anisotropy

The 48-layer symmetric homogeneous layups, with varying degrees of D_{16} and D_{26} coupling are as follows.

Layup A:
$(0, -45, 90, -45, 0, 45, 45, 90, -45, 90, 45, 45, 90,$
$0, 0, 90, 45, -45, 45, -45, 0, 0, 90, -45)_s$

Layup B:
$(0, -45, 90, -45, 0, -45, 45, 90, 45, 90, 45, 45, 90,$
$0, 0, 90, 45, -45, 45, -45, 0, 0, 90, -45)_s$

Layup C:
$(0, -45, 90, -45, 0, -45, -45, 90, 45, 90, 45, 45, 90,$
$0, 0, 90, 45, 45, 45, -45, 0, 0, 90, -45)_s$

Layup D:
$(0, -45, 90, -45, 0, -45, -45, 90, -45, 90, 45, 45,$
$90, 0, 0, 90, 45, 45, 45, 45, 0, 0, 90, -45)_s$

Layup E:
$(0, -45, 90, -45, 0, -45, -45, 90, -45, 90, -45,$
$45, 90, 0, 0, 90, 45, 45, 45, 45, 0, 0, 90, 45)_s$

Layup F:
$(0, -45, 90, 45, 0, -45, 45, 90, -45, 90, 45, -45, 90,$
$0, 0, 90, 45, -45, 45, 45, 0, 0, 90, -45)_s$

Layup G:
$(0, -45, 90, 45, 0, -45, -45, 90, 45, 90, -45, 45, 90,$
$0, 0, 90, 45, -45, 45, 45, 0, 0, 90, -45)_s$

Layup H:
$(0, -45, 90, 45, 0, -45, -45, 90, 45, 90, -45, 45,$
$90, 0, 0, 90, -45, -45, 45, 45, 0, 0, 90, 45)_s$

Layup I:
$(0, -45, 90, 45, 0, -45, -45, 90, 45, 90, -45, -45,$
$90, 0, 0, 90, 45, 45, 45, -45, 0, 0, 90, 45)_s$

Layup J:
$(0, -45, 90, -45, 0, -45, 45, 90, 45, 90, -45, -45,$
$90, 0, 0, 90, -45, 45, 45, 45, 0, 0, 90, 45)_s$

Layup K:
$(0, -45, 90, -45, 0, -45, -45, 90, 45, 90, -45, 45,$
$90, 0, 0, 90, -45, 45, 45, 45, 0, 0, 90, 45)_s$

Layup L:
$(-45, -45, -45, -45, 0, 90, 90, 90, 0, 0, 0, -45, 0,$
$90, 90, -45, 45, 45, 90, 45, 45, 0, 45, 45)_s$

Layup M:

$(-45, -45, -45, 0, -45, 90, 90, 90, 0, 0, 0, -45, -45, 90, 90, 45, 0, 0, 90, 45, 45, 45, 45, 45)s$

Layup N:

$(-45, -45, -45, -45, 90, 90, 0, 0, 0, 0, 90, -45, 90, 0, -45, 90, 45, 90, 45, 45, 0, 45, 45, 45)s$

Layup O:

$(-45, -45, -45, -45, 90, 90, 0, 0, 0, 90, -45, 90, 0, 0, 0, -45, 90, 45, 45, 45, 45, 90, 45, 45)s$

Layup P:

$(-45, -45, -45, 90, -45, 0, 0, 0, 45, 90, 90, 90, 0, 90, -45, 90, 0, 0, 45, 45, 45, 45, 45, 45)s$

Layup Q:

$(1)(-45, 45, -45, 45, 0, 90, 90, 90, 0, 0, 0, -45, 0, 90, 90, -45, 45, -45, 90, 45, 45, 0, 45, -45)s$

Layup R:

$(-45, -45, -45, 45, 0, 90, 90, 90, 0, 0, 0, 45, 0, 90, 90, -45, -45, 45, 90, 45, 45, 0, -45, 45)s$

Layup S:

$(-45, -45, -45, 0, 45, 90, 90, 90, 0, 0, 0, 45, -45, 90, 90, 45, 0, 0, 90, 45, 45, -45, -45, 45)s$

Layup T:

$(-45, -45, 45, 0, 45, 90, 90, 90, 0, 0, 0, 45, -45, 90, 90, -45, 0, 0, 90, -45, 45, 45, -45, 45)s$

Layup U:

$(45, -45, -45, -45, 90, 90, 0, 0, 0, 0, 90, 45, 90, 0, -45, 90, 45, 90, -45, 45, 0, 45, -45, 45)s$

Layup V:

$(-45, -45, -45, -45, 90, 90, 0, 0, 0, 0, 90, 45, 90, 0, 45, 90, -45, 90, 45, 45, 0, 45, 45, -45)s$

Layup W:

$(-45, -45, -45, -45, 90, 90, 0, 0, 0, 90, 45, 90, 0, 0, 0, 45, 90, -45, 45, 45, -45, 90, 45, 45)s$

Layup X:

$(45, -45, -45, -45, 90, 90, 0, 0, 0, 90, 45, 90, 0, 0, 0, -45, 90, 45, -45, -45, 45, 90, 45, 45)s$

Layup Y:

$(-45, -45, -45, 45, 90, 90, 0, 0, 0, 90, -45, 90, 0, 0, 0, 45, 90, 45, -45, 45, 45, 90, -45, 45)s$

Layup Z:

$(-45, -45, -45, -45, 90, 90, 0, 0, 0, 90, 45, 90, 0, 0, 0, 45, 90, 45, 45, 45, 45, 90, -45, -45)s$

Layup AA:

$(-45, -45, -45, -45, 90, 90, 0, 0, 0, 90, 45, 90, 0, 0, 0, -45, 90, 45, -45, 45, 45, 90, 45, 45)s$

Layup AB:

$(-45, -45, -45, -45, 90, 90, 0, 0, 0, 90, -45, 90, 0, 0, 0, 45, 90, 45, 45, 45, 45, 90, -45, 45)s$

Layup AC:

$(-45, -45, -45, -45, 0, 90, 90, 90, 0, 0, 0, -45, 0, 90, 90, 45, 45, 45, 90, 45, 45, 0, 45, -45)s$

Layup AD:

$(-45, -45, -45, 90, 45, 0, 0, 0, -45, 90, 90, 90, 0, 90, -45, 90, 0, 0, -45, 45, 45, 45, 45, 45)s$

Appendix C: Orthotropic Material Properties of T800-924 Carbon Fiber Reinforced Plastic (CFRP) Prepreg

Table C1 Orthotropic properties

Property	Value
E_{11}, GPa	161
E_{22}, GPa	11.5
G_{12}, GPa	7.170
ν_{12}	0.349

Appendix D: Buckling Loads of 48-Layer Homogeneous Laminates with D_{16} and D_{26} Coupling

Table D1 Buckling loads

Layup	Anisotropy factor (γ or δ)	Knockdown factor, k_D
A	0.018	0.984
B	0.042	0.958
C	0.104	0.890
D	0.156	0.834
E	0.198	0.788
F	0.032	0.969
G	0.053	0.945
H	0.067	0.931
I	0.085	0.911
J	0.120	0.873
K	0.155	0.835
L	0.239	0.725
M	0.243	0.718
N	0.243	0.719
O	0.245	0.716
P	0.253	0.703
Q	0.031	0.969
R	0.117	0.876
S	0.120	0.873
T	0.031	0.969
U	0.084	0.912
V	0.198	0.785
W	0.198	0.785
X	0.084	0.912
Y	0.137	0.855
Z	0.186	0.801
AA	0.209	0.769
AB	0.228	0.740
AC	0.222	0.750
AD	0.171	0.808

References

[1] Koiter, W. T., "The Stability of Elastic Equilibrium," Ph.D. Dissertation, Technische Hooge School, Delft, The Netherlands, 1945 (in Dutch); Riks, R., U.S. Air Force Flight Dynamics Lab., TR AFFDL-TR-70-25, Wright–Patterson AFB, OH, 1970 (English translation).

[2] Weaver, P. M., Driesen, J. R., and Roberts, P., "The Effect of Flexural-Twist Anisotropy on Compression Buckling of Quasi-Isotropic Laminated Cylindrical Shells," *Composite Structures*, Vol. 55, No. 2, 2002, pp. 195–204.

[3]Sobel, L. H., "Effects of Boundary Conditions on the Stability of Cylinders Subject to Lateral and Axial Pressures," *AIAA Journal*, Vol. 2, No. 8, 1964, pp. 1437–1440.

[4]Calladine, C. R., *Theory of Shell Structures*, Cambridge Univ. Press, New York, 1983, p. 229.

[5]Vasiliev, V. V., *Mechanics of Composite Materials*, Taylor and Francis, Philadelphia, 1993, p. 374.

[6]Weaver, P. M., and Dickenson, R. D., "Interactive Local/Euler Buckling of Orthotropic Cylindrical Shells," *Proceedings of International Conference on Composite Materials (ICCM13)*, Paper IO-1466, Beijing, 2001.

[7]Onoda, J., "Optimal Laminate Configuration of Cylindrical Shells for Axial Buckling," *AIAA Journal*, Vol. 23, No. 7, 1985, p. 1093.

[8]Fukunaga, H.,"Stiffness Optimization of Orthotropic Laminated Composites Using Lamination Parameters," *AIAA Journal*, Vol. 29, No. 4, 1991, pp. 641–646.

[9]Nemeth, M. P., "Importance of Anisotropy on Buckling of Composite-Loaded Symmetric Composites Plates," *AIAA Journal*, Vol. 24, No. 11, 1986, p. 1831.

[10]"ABAQUS User's Manual," Ver. 5.8, Hibbitt, Karlsson and Sorenson, Inc., Pawtucket, RI, 1999.

[11]Jaunky, N., and Knight, J. F., Jr., "An Assessment of Shell Theories for Buckling of Circular Cylindrical Panels Loaded in Compression," *International Journal of Solids and Structures*, Vol. 36, No. 25, 1999, pp. 3799–3820.

[12]Lord, G. J., Champneys, A. R., and Hunt, G. W., "Computation of Localised Post Buckling of Long Axially Compressed Cylinders," *Philosophical Transactions of the Royal Society of London, Series A: Mathematical and Physical Sciences,* Vol. 355, No. 1732, 1997, pp. 2137–2150.

[13]Lord, G. J., Champneys, A. R., and Hunt, G. W., "Computation of Homoclinic Orbits in Partial Differential Equations: an Application to Cylindrical Shell Buckling," *SIAM Journal on Scientific and Statistical Computing*, Vol. 21, No. 2, 1999, pp. 591–619.

[14]Batdorf, S. B., Stein, M., and Schilderout, M., "Critical Stresses of Thin-Walled Cylinder in Torsion," NACA TN 1344, 1947.

[15]Weaver, P. M., Driesen, J. R., and Roberts, P., "Anisotropic Effects in the Compression Buckling of Laminated Composite Cylindrical Shells," *Composites Science and Technology*, Vol. 62, No. 1, 2002, pp. 91–105.

[16]Reeves, A., and Weaver, P. M., "Imperfection Sensitivity of Composite Cylindrical Shells," Dept. of Aerospace Engineering, Rept. 924b, Univ. of Bristol, Bristol, England, U.K., May 2000.

[17]Hilburger, M. W., and Starnes, J. H., Jr., "Effect of Imperfections on the Buckling Response of Compression: Loaded Shells," AIAA Paper 2000-1387, April 2000.

E. R. Johnson
Associate Editor